Journal of Experimental Botany, Vol. 72, No. 22 pp. 7863–7875, 2021
https://doi.org/10.1093/jxb/erab372 Advance Access Publication 11 August 2021

RESEARCH PAPER

Dynamic changes in cell wall composition of mature sunflower leaves under distinct water regimes affect photosynthesis

Margalida Roig-Oliver[1,*], Panagiota Bresta[2], Dimosthenis Nikolopoulos[3], Josefina Bota[1], and Jaume Flexas[1,4]

[1] Research Group on Plant Biology under Mediterranean Conditions, Departament de Biologia, Universitat de les Illes Balears (UIB), INAGEA. Carretera de Valldemossa Km 7.5, 07122 Palma de Mallorca, Illes Balears, Spain.
[2] Laboratory of Electron Microscopy, Department of Crop Science, Agricultural University of Athens (AUA), Iera Odos 75, Botanikos, 11855 Athens, Greece.
[3] Laboratory of Plant Physiology and Morphology, Department of Crop Science, Agricultural University of Athens (AUA), Iera Odos 75, Botanikos, 11855 Athens, Greece.
[4] King Abdulaziz University, Jeddah, Saudi Arabia

* Correspondence: margaroig93@gmail.com

Received 10 May 2021; Editorial decision 3 August 2021; Accepted 9 August 2021

Editor: Johannes Kromdijk, University of Cambridge, UK

Abstract

In previous work, we identified that exposure to limited water availability induced changes in cell wall composition of mature *Helianthus annuus* L. leaves that affected mesophyll conductance to CO_2 diffusion (g_m). However, it is unclear on which timescale these changes in cell wall composition occurred. Here, we subjected *H. annuus* to control (i.e. water availability), different levels of short-term water deficit stress (ST), long-term water deficit stress (LT), and long-term water deficit stress followed by gradual recoveries addressed at different timescales (LT-Rec) to evaluate the dynamics of modifications in the main composition of cell wall (cellulose, hemicelluloses, pectins and lignins) affecting photosynthesis. During gradual ST treatments, pectins enhancement was associated with g_m decline. However, during LT-Rec, pectins content decreased significantly after only 5 h, while hemicelluloses and lignins amounts changed after 24 h, all being uncoupled from g_m. Surprisingly, lignins increased by around 200% compared with control and were related to stomatal conductance to gas diffusion (g_s) during LT-Rec. Although we suspect that the accuracy of the protocols to determine cell wall composition should be re-evaluated, we demonstrate for the first time that a highly dynamic cell wall composition turnover differently affects photosynthesis in plants subjected to distinct water regimes.

Keywords: Cell wall composition, *Helianthus annuus*, lignins, mesophyll conductance to CO_2 diffusion, pectins, photosynthesis, recovery, stomatal conductance to gas diffusion, water deficit stress.

Abbreviations: AIR, Alcohol insoluble residue; A_N, net CO_2 assimilation; ETR, electron transport rate; g_m, mesophyll conductance to CO_2 diffusion; g_s, stomatal conductance to gas diffusion; R_{light}, light mitochondrial non-photorespiratory respiration rate; RWC, leaf relative water content; WUE, water use efficiency; ψ, leaf water potential; ψ_{md}, midday leaf water potential; ψ_{pd}, pre-dawn leaf water potential.

Introduction

The plant cell wall is a complex structure surrounding plant cells that is composed of distinct types of polysaccharides, phenolic compounds, structural proteins, and other small molecules (Carpita and Gibeaut, 1993; Cosgrove, 2005; 2018; Keegstra, 2010; Tenhaken, 2015; De Lorenzo *et al.*, 2019; Anderson and Kieber, 2020). Most studies have focused on primary cell walls, which are mainly formed by cellulose, hemicelluloses, and pectins (Carpita and Gibeaut, 1993; Cosgrove, 2005; 2018; Tenhaken, 2015; Novaković *et al.*, 2018; De Lorenzo *et al.*, 2019; Anderson and Kieber, 2020). Of these, cellulose is the most abundant polysaccharide, consisting of a few 100 to over 10 000 residues of (1,4)-linked-β-D-glucose chains forming long, insoluble, and unbranched crystalline microfibrils due to hydrogen bonds (Cosgrove, 2005; 2018; Keegstra, 2010; Anderson and Kieber, 2020). Among those closely packed cellulose microfibrils, non-cellulosic polysaccharides (hereafter referred as hemicelluloses) are deposited (Carpita and Gibeaut, 1993; Tenhaken, 2015; Novaković *et al.*, 2018). This cellulose-hemicelluloses network is entrenched in a pectin matrix which is thought to be a crucial structure determining cell wall hydrophilic properties as well as its porosity, viscosity, rigidity, and thickness (Baron-Epel *et al.*, 1988; Vicré *et al.*, 1999; Cosgrove, 2005; Moore *et al.*, 2008; Ochoa-Villarreal *et al.*, 2012; Houston *et al.*, 2016; Carriquí *et al.*, 2020; Roig-Oliver *et al.*, 2020a, b, c). In some types of primary cell walls, secondary walls are internally deposited to provide strength and rigidity to tissues that are no longer growing (Cosgrove, 2005; Keegstra, 2010; Tucker *et al.*, 2018). In particular, lignin is a specific phenolic polymer relatively abundant in secondary walls (Iiyama *et al.*, 1994; Wallace and Fry, 1994). It is compounded by highly condensed polymeric matrices, which conform the core lignin, and by low molecular weight phenolic monomers and oligomers, representing the non-core lignin (Moreira-Vilar *et al.*, 2014). Lignin accumulation during plant exposure to environmental stresses has been related to alterations in cell wall characteristics, such as extensibility, hydrophobicity, flexibility, and mechanical strength (Iiyama *et al.*, 1994; Wallace and Fry, 1994; Lampugnani *et al.*, 2018; Terrett and Dupree, 2019).

The cell wall was traditionally considered to be robust and static from a compositional perspective, but it is now recognized as a highly dynamic structure that is required to define leaf architecture (Baskin, 2005; Cosgrove, 2005; 2018; Caffall and Mohnen, 2009; Ochoa-Villarreal *et al.*, 2012; Tenhaken, 2015; Lampugnani *et al.*, 2018; Weraduwage *et al.*, 2018; De Lorenzo *et al.*, 2019; Rui and Dinneny, 2019; Anderson and Kieber, 2020). In particular, modifications in the cell wall occur during its synthesis and assembly, promoting changes in the orientation of cytoskeleton structures with subsequent alterations in the cross-linking interactions between cell wall components (Weraduwage *et al.*, 2018). However, there is still controversy when referring to the dynamics of those modifications occurring in the cell wall of expanded and mature leaves (Houston *et al.*, 2016; Cosgrove, 2018). It is assumed that changes in cell wall composition and architecture control different stages of plant cell differentiation during embryogenesis and subsequent growth (Cosgrove, 2018), leading to the establishment of a specific leaf architecture (Weraduwage *et al.*, 2018). Thus, during cell growth, the cell wall has to be flexible enough to allow for cellular expansion and it has to synthesize new wall material to properly encapsulate and reinforce the growing cell while providing structural support (Baskin, 2005; Houston *et al.*, 2016; Lampugnani *et al.*, 2018; Weraduwage *et al.*, 2018). Hence, the genetic regulation of the constant synthesis and modification of the cell wall material promotes disruptions and cross-linkage reassembly (Cosgrove, 2005; 2018; Weraduwage *et al.*, 2018). However, when the cell has ceased growing and dividing and leaves are fully expanded, thicker and robust secondary walls are internally deposited in some types of primary walls (Cosgrove, 2005; Keegstra, 2010; Houston *et al.*, 2016; Lampugnani *et al.*, 2018; Tucker *et al.*, 2018). In these mature leaves, cell wall composition modifications were thought to be of lesser importance in comparison to those taking place during leaf growth and expansion (Houston *et al.*, 2016; Cosgrove, 2018), inhibiting wall ability to rearrange in response to external stressors (Sahaf and Sharon, 2016).

Some studies have recently demonstrated that mature leaves of plants subjected to different abiotic stressors display significant changes in their cell wall composition that are strongly related to photosynthesis – particularly, to mesophyll conductance to CO_2 diffusion (g_m)–, suggesting that these modifications may dynamically affect cell wall porosity in response to stress (Clemente-Moreno *et al.*, 2019; Roig-Oliver *et al.*, 2020a, c). Although specific differences were found depending on the tested species and stress conditions, in most of these studies the pectins content or the pectins fraction was positively or negatively correlated with g_m, suggesting that they could be of special relevance determining cell wall properties affecting CO_2 diffusion and thus, g_m (Flexas *et al.*, 2021). Regardless of the specific relationship between g_m and cell wall composition found in these previous studies, all of the analysed photosynthesis and cell wall composition responses after plants acclimation to a particular condition from days to weeks. Therefore, it remains unexplored if the speed of those modifications occurring in the cell wall composition of mature leaves could also determine photosynthesis in a shorter timeframe.

Since the application of distinct water availability regimes induces changes in both photosynthesis and cell wall composition (Vicré *et al.*, 1999; Chaves *et al.*, 2002; 2009; Flexas *et al.*, 2004; Tenhaken, 2015; Novaković *et al.*, 2018; Rui and Dinneny, 2019; Roig-Oliver *et al.*, 2020a, c), we subjected *Helianthus annuus* L. to different water conditions with two aims: (i) to confirm the relevance of these cell wall modifications affecting photosynthesis in an extended range of short-term water deficit stress conditions; and (ii) to evaluate the dynamics of those changes occurring in the cell wall composition of mature leaves immediately after rewatering plants subjected to long-term water deficit stress. Thus,

we extended the experimental design of our previous study in the same species (Roig-Oliver *et al.*, 2020a) by applying gradual short-term water deficit stress treatment and a long-term water deficit stress treatment followed by gradual recovery, to monitor in detail how modifications in the main composition of cell walls (i.e. cellulose, hemicelluloses, pectins, and lignins) and photosynthesis occurred.

Material and methods

Plant material, experimental design, and growth conditions

Helianthus annuus seeds were sown individually in water-irrigated 3 l pots containing a substrate mixture of peat: perlite (3:1, v/v). They were placed in a growth chamber at 25 °C receiving 200–300 μmol m^{-2} s^{-1} of photosynthetic photon flux density (PPFD) for 12 h followed by 12 h of darkness. On the sowing day, pots were randomly subjected to different growing conditions: control (CL, without stress), short-term water deficit stress (ST), long-term water deficit stress (LT) and long-term water deficit stress followed by a recovery (LT-Rec). Within the plants belonging to ST and LT-Rec treatments, randomly selected individual replicates were kept under distinct water availability conditions for a detailed monitoring of those changes associated with specific levels of ST and LT-Rec (see Fig. 1 for more detail).

Control plants were maintained at 100% field capacity (FC) for 44 d. The same conditions were applied to all plants belonging to ST treatments, followed by the application of water deprivation. In order to monitor those changes occurring immediately after achieving a specific level of water shortage, individual ST replicates were randomly selected to be measured when reaching 80, 65, 50 and 40% FC (named ST-80% FC, ST-65% FC, ST-50% FC and ST-40% FC, respectively; Fig. 1). As it took 4 d to descend from a specific level of FC to the following, additional control plants were maintained at 100% FC during the gradual performance of ST. Thus, they were measured at the same ages of ST-65% FC and ST-40% FC treatments (i.e. 52 and 60 days-old, respectively; Fig. 1) to remove the 'age effect' from all ST measurements, ensuring that photosynthetic and cell wall compositional changes were exclusively attributed to each specific level of water deficit stress. LT treatment was achieved by decreasing the pots FC from 100% to 40%, starting at the sowing day. Hence, when 40% FC was reached – usually after 18 d from sowing–, this water status was maintained for 26 d. Plants belonging to LT-Rec treatments were kept under the same conditions as those of LT, but a rewatering to 100% FC was applied at different time points to ensure that all of them were 44 days old when measured. Specifically, plants were recovered and subsequently maintained at 100% FC for 5, 24, 48, 72 and 96 h (LT-Rec 5 h, LT-Rec 24 h, LT-Rec 48 h, LT-Rec 72 h and LT-Rec 96 h, respectively; Fig. 1). Considering that no leaves were unfolded during ST treatments, measurements were performed on fully expanded leaves previously developed under well-watered conditions. Instead, LT treatment allowed for expansion of leaves under stress conditions. Thus, LT and LT-Rec measurements were performed in fully expanded leaves developed under water shortage.

In all cases, five randomly selected individual replicates were subjected to those specific conditions imposed by each treatment (Fig. 1). All plants were monitored daily to maintain each pot FC at a specific level by replacing evapo-transpired water.

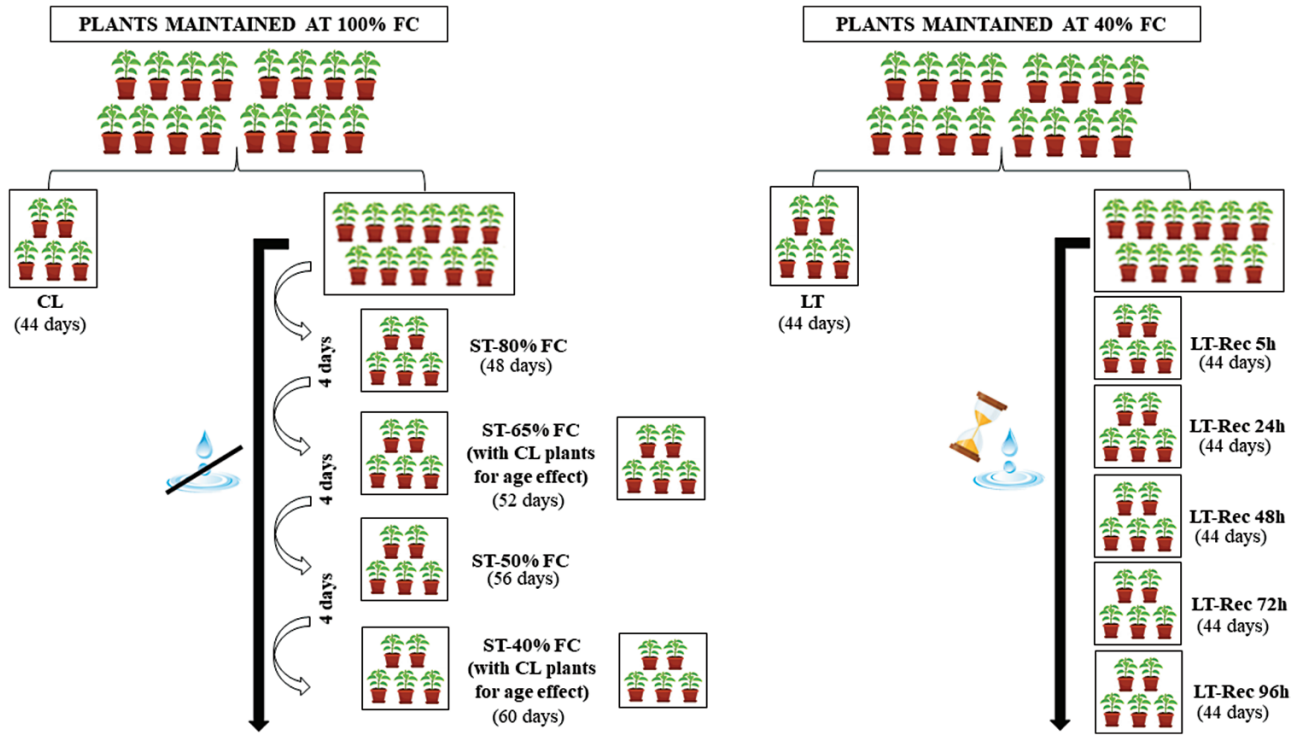

Fig. 1. Diagram representing the experimental design of the study. Specific growing conditions for all plants subjected to each treatment are shown (CL: control; ST-80%, ST-65% FC, ST-50% FC and ST-40% FC: short-term water deficit stress at 80%, 65%, 50% and 40% field capacity (FC), respectively; LT: long-term water deficit stress; LT-Rec 5 h, LT-Rec 24 h, LT-Rec 48 h, LT-Rec 72 h and LT-Rec 96 h: long-term water deficit stress followed by 5, 24, 48, 72 and 96 h of recovery, respectively). Also, the age of the plants when measured is included. Whilst water drops represent water shortage or water supply in ST or LT-Rec treatments, respectively, the timer indicates that the watering was addressed at different moments during LT-Rec. *n*=5 in all treatments.

Plant water status

For each plant belonging to CL, LT and ST treatments, a fully expanded leaf was used to determine the pre-dawn (ψ_{pd}) and the midday (ψ_{md}) leaf water potentials with a pressure chamber (Model 600D; PMS Instrument Company, Albany, USA). Instead, the leaf water potential (ψ) was determined before starting gas exchange performance in all LT-Rec treatments. Additionally, the leaf relative water content (RWC) was calculated in the same leaves in which ψ_{md} and ψ were estimated using the following equation:

$$RWC = \frac{FW - DW}{TW - DW} \quad x \quad 100$$

Thus, leaves' fresh weight (FW) was obtained immediately after measuring ψ_{md} or ψ. Then, leaves' turgid weight (TW) was obtained after their rehydration in distilled water for 24 h in darkness at 4 °C. Finally, leaves were transferred to an oven kept at 70 °C for, at least 72 h, to obtain their dry weight (DW).

Gas exchange and chlorophyll fluorescence measurements

A gas exchange system equipped with a 2 cm^2 fluorescence chamber (Li-6400-40; Li-Cor Inc., Lincoln, NE, USA) was used to perform simultaneous measurements of gas exchange and chlorophyll *a* fluorescence. For each plant, the third fully expanded leaf from the apex was used to determine the net CO_2 assimilation (A_N), the stomatal conductance to gas diffusion (g_s), the CO_2 concentration at the sub-stomatal cavity (C_i) and the steady-state fluorescence (F_s) at 25 °C, 400 μmol CO_2 mol^{-1} air and saturating light (1500 μmol m^{-2} s^{-1}, 90–10% red-blue light) after reaching steady-state conditions (usually after 15–20 min). Subsequently, a saturating light flash of around 8000 μmol m^{-2} s^{-1} was applied to determine the maximum fluorescence (F_m'). From these values, the real quantum efficiency of photosystem II (Φ_{PSII}) was recorded in the equipment. The electron transport rate (ETR) was calculated as described in Valentini *et al.* (1995) by the performance of light curves under negligible photorespiratory conditions (≃ 1% O_2). The dark respiration rate was estimated after plants acclimation to darkness for 30 min (Niinemets *et al.*, 2005). The light mitochondrial non-photorespiratory respiration rate (R_{light}) was assumed to be half the dark respiration rate. The mesophyll conductance to CO_2 diffusion (g_m) was estimated from previous values (Harley *et al.*, 1992), assuming that the CO_2 compensation point in the absence of respiration ($\Gamma^\star$) was averaged from previously reported values for *H. annuus* (Parry *et al.*, 1989; Kent *et al.*, 1992; Kanevski *et al.*, 1999; Sharwood *et al.*, 2008), corresponding to 40.65 μmol CO_2 mol^{-1} air. Thus, the following equation was used:

$$g_m = \frac{A_N}{C_i - \frac{\Gamma^*((ETR+8(A_N+R_{light}))}{ETR-4(A_N+R_{light})}}$$

Cell wall extraction and fractionation

Sampling for cell wall composition analyses was done in the same leaves used for gas exchange measurements. Whereas in CL, LT, and all ST treatments the sampling was performed after keeping plants under darkness overnight to minimize foliar starch content, LT-Rec sampling was addressed immediately after completing gas exchange measurements. In all cases, around 1 g of fresh foliar tissue per plant was cut avoiding the main veins. These portions were placed in screw-capped glass tubes filled with absolute ethanol (i.e. 100%) to be boiled until bleached. In order to eliminate any alcohol-soluble residue, samples were cleaned twice with acetone >95% for 30 min, obtaining the alcohol insoluble residue (AIR), an approximation of the crude isolated cell wall material. Each AIR was split in two for the evaluation of distinct cell wall compounds. The AIR fraction destined to cellulose, hemicelluloses and pectins quantification was subjected to α-amylase digestion to remove starch residues, which were especially abundant in LT-Rec treatments due to sampling conditions. When no starch residues were further observed, three technical replicates per AIR weighing around 3 mg were hydrolysed with 2 M trifluoroacetic at 121 °C for 1 h. They were subsequently centrifuged at 13 000 × *g*, differentiating an aqueous supernatant (non-cellulosic cell wall material, i.e. hemicelluloses and pectins) and a pellet (cellulosic cell wall material). Although supernatants were kept at –20 °C until use, cellulosic pellets were cleaned twice with distilled water and twice more with acetone >95%. They were air-dried at 25 °C to be hydrolysed with 200 μl of 72% (w/v) sulphuric acid for 1 h, diluted to 6 ml with distilled water, and heated at 121 °C until the pellet degraded. Once cooled, the obtained aqueous samples were used for cellulose quantification following the phenol sulphuric acid method (Dubois *et al.*, 1956). The same procedure was used to calculate the concentration of hemicelluloses. Thus, the concentration of both sugars was estimated by interpolating sample absorbance at 490 nm from a glucose calibration curve. To quantify pectins, sample absorbance was read at 520 nm to be calculated from a galacturonic acid calibration curve (Blumenkrantz and Asboe-Hansen, 1973). In all cases, a Multiskan Sky Microplate Spectrophotometer (ThermoFisher Scientific, USA) was used. The remaining AIR fraction used for lignins quantification was dehydrated in an oven at 70 °C for at least 72 h. AIRs were ground to a fine powder and around 15 mg of each sample was used to quantify lignins content using the acetyl bromide method (Fagerstedt *et al.*, 2015), which quantifies both core and non-core lignins (Moreira-Vilar *et al.*, 2014). Hence, lignins concentration was obtained by interpolating sample absorbance at 280 nm from a lignin calibration curve. In this case, a UV-160A Shimadzu spectrophotometer (Shimadzu Corp., USA) was used.

Statistical analysis

Before any other statistical analysis, Thompson test was applied to find and subtract outliers for all studied parameters. After that, R software (ver. 3.2.2; R Core Team, Vienna, Austria) was used to perform further statistical tests. First, data passed Shapiro–Wilk and Bartlett tests for normality and equality of variances, respectively. Next, one-way ANOVA and subsequent LSD test were used to detect statistically significant differences ($P \leq 0.05$) among treatments during gradual ST and during LT with gradual recoveries for all tested parameters. Subsequently, Pearson's correlation matrices were created to find pair-wise correlations among all analysed parameters, being significant and highly significant at $P \leq 0.05$ and $P \leq 0.01$, respectively. Finally, linear regressions between photosynthetic features and cell wall compositional traits were fitted utilizing mean values per treatment.

Results

Physiological and cell wall compositional changes in response to gradual levels of short-term water deficit stress

The application of ST treatments resulted in statistically significant lower values for ψ_{pd}, ψ_{md} and RWC than under CL ($P<0.01$ in all cases; Table 1). In particular, ψ_{pd} decreased gradually when intensifying the level of water shortage until reaching the lowest value in ST-40% FC (–1.69±0.07 MPa; Table 1). Although ψ_{md} was similarly maintained to CL in ST-80% FC and ST-65% FC, significant reductions ($P<0.01$) were found under ST-50% FC (Table 1). Again, ST-40% FC presented the lowest value (–1.89±0.11 MPa; Table 1). Whilst CL and ST-80% FC exhibited the highest RWC, ST-40% FC reached the lowest value (44.59±2.51%; Table 1).

Table 1. Leaf water status of *H. annuus* plants gradually subjected to different conditions.

Treatments	Ψ_{pd} (MPa)	Ψ_{md} (MPa)	RWC (%)
CL	-0.12±0.01^{a}	-0.27±0.06^{a}	84.54±0.57^{a}
ST-80% FC	-0.20±0.02^{ab}	-0.35±0.05^{a}	81.17±0.62^{a}
ST-65% FC	-0.29±0.05^{b}	-0.36±0.05^{a}	79.86±0.68^{b}
ST-50% FC	-0.54±0.07^{c}	-0.95±0.08^{b}	81.99±0.82^{ab}
ST-40% FC	-1.69±0.07^{d}	-1.89±0.11^{c}	44.59±2.51^{c}

Treatments' abbreviations correspond to CL: control; ST-80%, ST-65% FC, ST-50% FC and ST-40% FC: short-term water deficit stress at 80%, 65%, 50% and 40% FC, respectively. Mean values ± SE are shown for pre-dawn leaf water potential (Ψpd), midday leaf water potential (Ψmd), and leaf relative water content (RWC). Different letters indicate significant difference ($P \leq 0.05$) across all experimental conditions according to LSD test. $n=5$ in all cases.

ST application did not result in a statistically significant decrease in A_N compared with CL until reaching ST-40% FC (3.54±0.51 μmol CO_2 m^{-2} s^{-1}; Table 2). CL presented the highest g_s (0.33±0.06 mol CO_2 m^{-2} s^{-1}), which was reduced up to 80% after ST-40% FC application (Table 2). Concerning g_m, slight reductions were promoted during gradual ST, achieving the lowest value in ST-40% FC (0.09±0.00 mol CO_2 m^{-2} s^{-1}; Table 2). Similarly, only ST-40% FC displayed significantly increased WUE compared with CL ($P<0.01$; Table 2). No statistically significant differences were found among treatments for ETR and R_{light} ($P=0.96$ and 0.41, respectively; Table 2).

Based on absolute values for each cell wall component (Supplementary Table S1), the timescale variation in their relative abundance during gradual ST application is shown (Fig. 2). Whilst the relative abundance of cellulose was gradually reduced from CL to ST-65% (i.e. from 100±11.42 to 45.43±3.29% CL), significant enhancements were subsequently detected ($P<0.01$; Fig. 2). Although the relative content of hemicelluloses was maintained at values close to CL in ST-80% FC, it dropped thereafter, presenting similarly lower values across ST-65%, 50% and 40% FC (Fig. 2). The relative concentration of pectins increased during gradual ST, reaching the highest value in ST-40% FC (165.87±9.76% CL; Fig. 2). Even though the relative abundance of lignins was almost maintained at CL in ST-80% FC and ST-65% FC (116.31±5.94 and 110.74±9.66% CL, respectively), reductions of around 37% were detected in ST-50% FC, compared with CL (Fig. 2). Nonetheless, ST-40% FC presented almost 1.3 times higher relative concentration of lignins compared with CL (Fig. 2).

All the results described above were obtained after subtracting the age effect in all ST treatments by measuring plants kept at 100% FC that presented the same age as those belonging to ST-65% FC and ST-40% FC (Fig. 1). The obtained data was normalized with a calibration curve allowing for calculation of the age effect, which was subtracted from all the data obtained in ST measurements. However, the trends were similar for all parameters even without correcting the data (Supplementary Fig. S1; Supplementary Tables S2; S3). Significant correlations between photosynthetic and cell wall composition parameters expressed on an AIR basis were detected during gradual ST application (Supplementary Table S4). Particularly, whilst g_m and pectins correlated negatively ($R^2=0.7$, $P=0.05$, Fig. 3A), a positive relationship between the g_m/g_s ratio and pectins was found ($R^2=0.91$, $P<0.01$, Fig. 3B). Nonetheless, these correlations were non-significant when expressing pectins on an area basis ($R^2=$–0.29, $P=0.77$ and $R^2=0.19$, $P=0.26$, Figs. 3C, D, respectively).

Physiological and cell wall compositional changes upon long-term water deficit stress and subsequent recovery

Although LT presented the lowest ψ among treatments (–1.68±0.30 MPa), it was immediately restored to CL upon recovery (Fig. 4A). Similarly, LT presented the lowest RWC (55.68±0.96%), which increased gradually during LT-Rec application until restoring CL value in LT-Rec 48 h (Fig. 4B).

The application of LT-Rec treatments resulted in gradual photosynthesis enhancement since LT-Rec 96 h presented almost 2.5 times larger A_N than CL (31.40±1.57 μmol CO_2 m^{-2} s^{-1}; Fig. 5A). Regarding g_s, CL value was achieved in LT-Rec 24 h (0.33±0.05 mol CO_2 m^{-2} s^{-1}) and increased thereafter until reaching the highest value in both LT-Rec 72 h and LT-Rec 96 h (Fig. 5B). Nonetheless, LT and LT-Rec treatments did not promote any statistically significant modification for g_m compared with CL (Fig. 5C). However, LT-Rec 5 h application declined WUE by around 23% in comparison to LT (Fig. 5D). Further reductions were detected in LT-Rec 24 h and thereafter, representing the achievement of CL value (Fig. 5D). The highest ETR was exhibited in both LT-Rec 72 h and LT-Rec 96 h treatments (243.10±13.14 and 274.55±20.93 μmol m^{-2} s^{-1}, respectively), representing more than 2–fold larger ETR than CL (Fig. 5E). Finally, R_{light} gradually increased during LT-Rec application, reaching the highest value in LT-Rec 72 h (1.81±0.16 μmol CO_2 m^{-2} s^{-1}; Fig. 5F).

Absolute values for each cell wall component are shown in Supplementary Table S1. Concerning the timescale variation in cell wall composition during LT and gradual LT-Rec application, the relative concentration of cellulose was equally maintained to CL values across all tested conditions (Fig. 6). Nonetheless, LT and subsequent LT-Rec treatments resulted in significantly lower ($P<0.01$) relative abundance of hemicelluloses compared with CL (Fig. 6). Although LT exhibited higher relative concentration of pectins than CL (123.70±3.64 versus 100.00±4.82% CL, respectively), it was significantly reduced ($P<0.01$) upon recovery, finally reaching an almost similar CL value in LT-Rec 96h (87.82±1.54% CL; Fig. 6). The relative abundance of lignins was around 3.5–fold lower in both LT and LT-Rec 5 h, compared with CL (Fig. 6). However, the relative abundance of lignins increased up to 200% in LT-Rec 24 h, 48 h, 72 h, and 96 h (Fig. 6).

Significant relationships between photosynthetic and cell wall composition parameters either expressed on an AIR or on

Table 2. Photosynthetic characterization of *H. annuus* plants gradually subjected to different conditions.

Treatments	A_N (μmol CO_2 m^{-2} s^{-1})	g_s (mol CO_2 m^{-2} s^{-1})	g_m (mol CO_2 m^{-2} s^{-1})	WUE (μmol CO_2 mol^{-1} H_2O)	ETR (μmol m^{-2} s^{-1})	R_{light} (μmol CO_2 m^{-2} s^{-1})
CL	13.92±0.37^{a}	0.33±0.06^{a}	0.18±0.03^{a}	52.08±1.82^{b}	101.74±4.71^{a}	0.93±0.15^{a}
ST-80% FC	10.61±2.36^{a}	0.14±0.03^{bc}	0.12±0.02^{bc}	66.65±5.13^{b}	103.61±18.48^{a}	1.10±0.18^{a}
ST-65% FC	9.69±1.26^{a}	0.19±0.04^{bc}	0.14±0.01^{ab}	69.46±6.90^{b}	90.57±0.84^{a}	1.09±0.09^{a}
ST-50% FC	11.37±1.03^{a}	0.21±0.04^{b}	0.13±0.01^{abc}	69.11±5.86^{b}	102.11±2.29^{a}	0.78±0.11^{a}
ST-40% FC	3.54±0.51^{b}	0.06±0.00^{c}	0.09±0.00^{c}	110.28±12.07^{a}	92.26±18.96^{a}	0.88±0.14^{a}

Treatments' abbreviations correspond to CL: control; ST-80%, ST-65% FC, ST-50% FC and ST-40% FC: short-term water deficit stress at 80%, 65%, 50% and 40% FC, respectively. Mean values ± SE are shown for net CO_2 assimilation (A_N), stomatal conductance to gas diffusion (g_s), mesophyll conductance to CO_2 diffusion (g_m), water use efficiency (WUE), electron transport rate (ETR), and light mitochondrial non-photorespiratory respiration rate (R_{light}). Different letters indicate significant difference ($P \leq 0.05$) across all experimental conditions according to LSD test. $n=5$ in all cases.

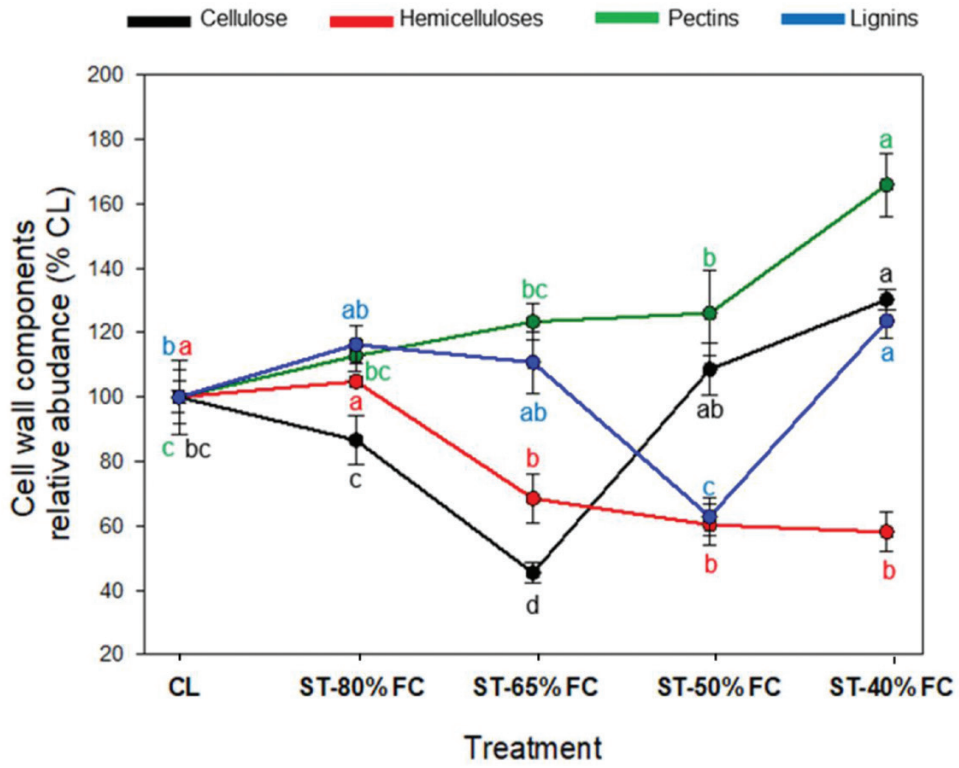

Fig. 2. Relative abundance of main cell wall components during gradual ST application. Treatments' abbreviations correspond to CL: control; ST-80%, ST-65% FC, ST-50% FC and ST-40% FC: short-term water deficit stress at 80%, 65%, 50% and 40% field capacity (FC), respectively. Different letters indicate significant difference ($P \leq 0.05$) across all experimental conditions according to LSD test. $n=5$ (means ± SE).

an area basis were found during LT and gradual LT-Rec treatments (Supplementary Table S5). Specifically, a positive correlation between g_s and lignins expressed on an AIR basis was detected ($R^2=0.69$, $P=0.01$; Fig. 7A), while expressing lignins on an area basis resulted in an increase in the strength of the correlation ($R^2=0.74$, $P<0.01$; Fig. 7B).

Discussion

The application of distinct water availability regimes affect photosynthesis differently

Water availability is crucial for plant development, growth, and survival (Chaves *et al.*, 2002; 2009; Flexas *et al.*, 2004). Since the intensity and the duration of distinct water shortage conditions promote different photosynthetic adjustments (Chaves *et al.*, 2009), we reported contrasting responses due to ST and LT application. Although A_N reduction during gradual ST mainly resulted from a g_s decline (Table 2), LT reached higher A_N rates than control because of an enhancement in ETR and g_m (Fig. 5). These results show a clear acclimation response in sunflower leaves that emerged after LT application, and agree with the observed results from previous studies in the same species (Pankovi ć *et al.*, 1999; Roig-Oliver *et al.*, 2020a). Nonetheless, gradual photosynthesis enhancement during LT-Rec treatments was attributed to stomatal opening as well as an increase in biochemical capacity (Fig. 5).

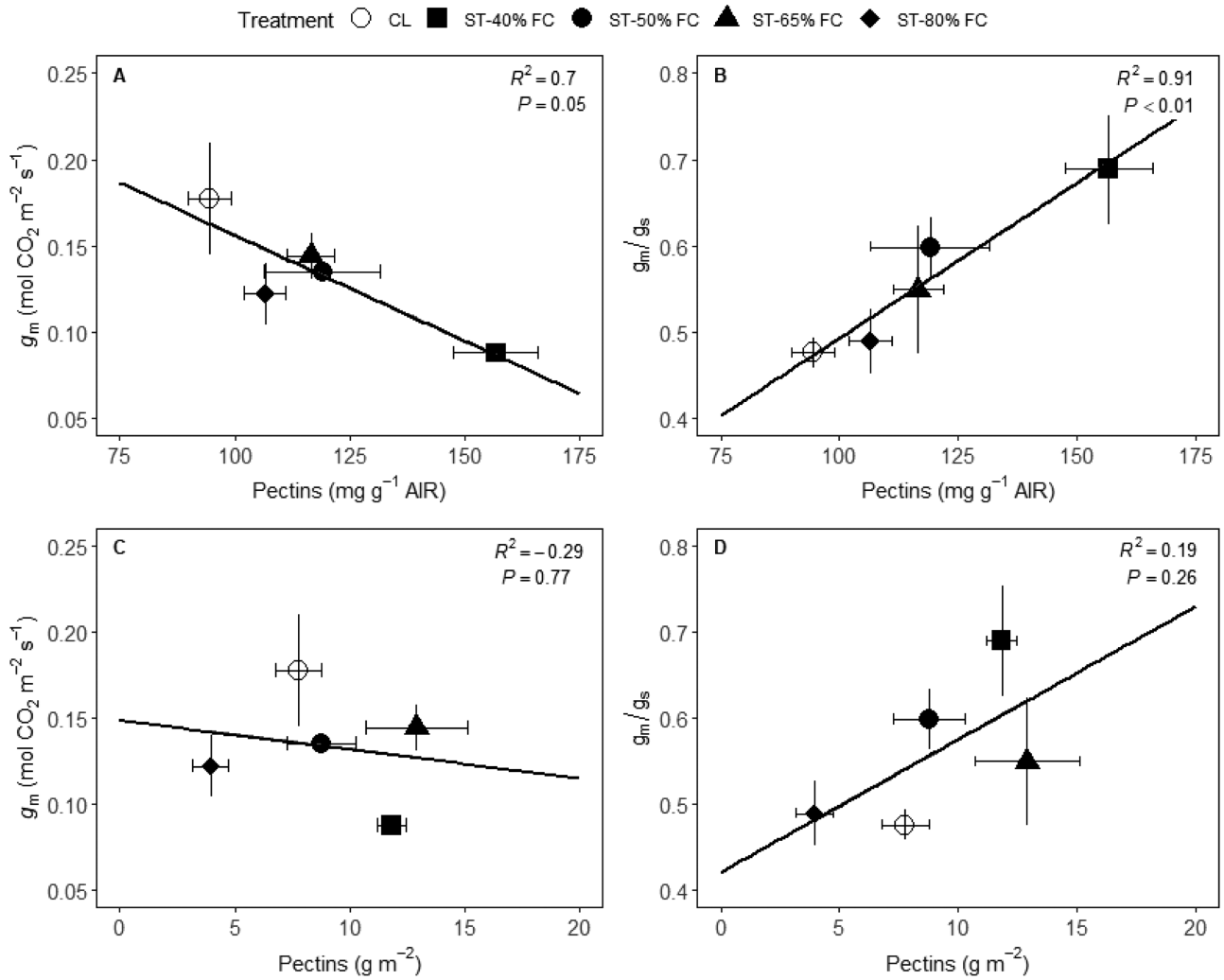

Fig. 3. Cell wall composition in relation to photosynthesis during gradual short-term water deficit stress application. Relationship between mesophyll conductance to CO_2 diffusion (g_m) and pectins content expressed on an AIR basis (A), and relationship between the g_m/g_s ratio and pectins content expressed on an AIR basis (B). Relationship between mesophyll conductance to CO_2 diffusion (g_m) and pectins content expressed on an area basis (C), and relationship between the g_m/g_s ratio and pectins content expressed on an area basis (D). n=5 (means ± SE).

Discrepancies between expressing cell wall composition on an area or on an AIR basis

Although the colorimetric protocols that we utilized are well contrasted and often used (Ibarz *et al.*, 2005; Masuko *et al.*, 2005; Moreira-Vilar *et al.*, 2014), the obtained results show a consistent discrepancy with the general idea that the sum of cellulose, hemicelluloses and pectins represents the main primary cell wall (Carpita and Gibeaut, 1993; Cosgrove, 2005; 2018; Tenhaken, 2015; De Lorenzo *et al.*, 2019; Anderson and Kieber, 2020). This fact suggests that, even being widely accepted, the accuracy of these methods should be further analysed and re-evaluated, which in turn may require re-evaluation of the main conclusions of those studies in which these protocols were used. Despite this, since calibration curves were performed in triplicate in each reaction ensuring high regression coefficients (R^2 >0.989 in all cases), we are confident that our results reflect the contents of each analysed cell wall compound at least in a semi-quantitative manner.

When using these methods, the concentration of cell wall components is often expressed on an AIR basis instead of an area or dry mass basis (Rancour *et al.*, 2012; Uddin *et al.*, 2014; Clemente-Moreno *et al.*, 2019; Nadal *et al.*, 2020; Roig-Oliver *et al.*, 2020a, b, c). In fact, differences between expressing values on an AIR or on an area basis could be attributed to different facts. Whilst larger AIR per leaf area could represent cell wall thickening and, thus, decreased g_m, it would also correspond to increased leaf thickness at constant cell wall composition, which may enhance g_m. In this regard, if the major role of cell wall composition in relation to photosynthesis is to define cell wall porosity, it might be more appropriate to express cell wall compounds on an AIR basis or even as a ratio between them, since it is the proportion rather than their

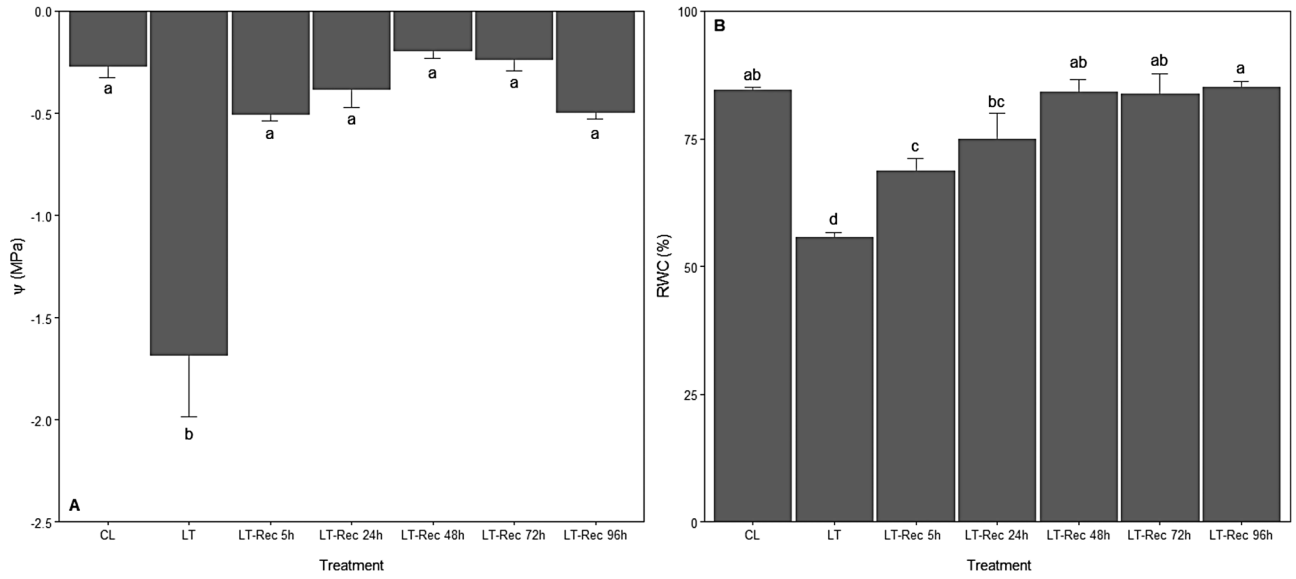

Fig. 4. Recovery of leaf water status of *H. annuus* plants. Treatments' abbreviations correspond to CL: control; LT: long-term water deficit stress; LT-Rec 5 h, LT-Rec 24 h, LT-Rec 48 h, LT-Rec 72 h, and LT-Rec 96 h: long-term water deficit stress followed by 5, 24, 48, 72 and 96 h of recovery, respectively. Mean values ± SE are shown for (A) leaf water potential (Ψ) and (B) leaf relative water content (RWC). Different letters indicate significant difference ($P \leq 0.05$) across all experimental conditions according to LSD test. $n=5$ in all cases.

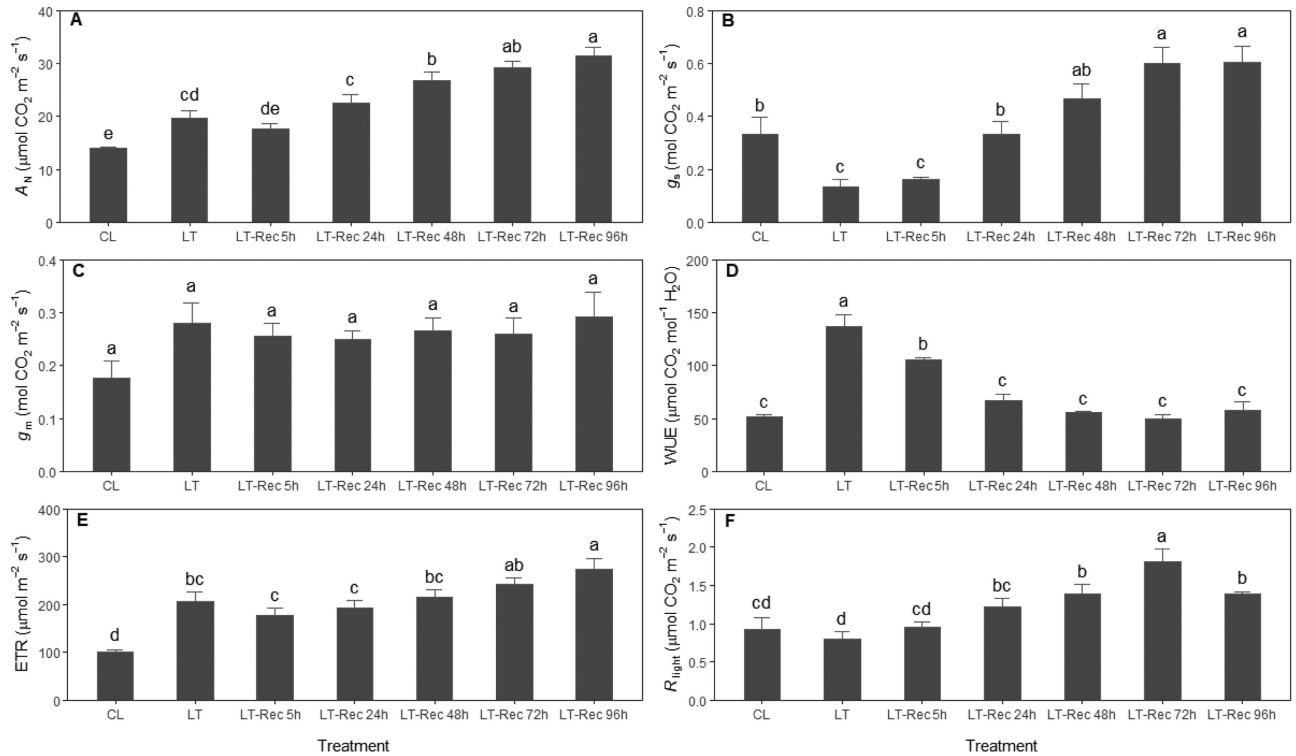

Fig. 5. Recovery of photosynthetic parameters in *H. annuus* plants. Treatments' abbreviations correspond to CL: control; LT: long-term water deficit stress; LT-Rec 5 h, LT-Rec 24 h, LT-Rec 48 h, LT-Rec 72 h and LT-Rec 96 h: long-term water deficit stress followed by 5, 24, 48, 72 and 96 h of recovery, respectively. Mean values ± SE are shown for (A) net CO_2 assimilation (A_N); (B) stomatal conductance to gas diffusion (g_s); (C) mesophyll conductance to CO_2 diffusion (g_m); (D) water use efficiency (WUE); (E) electron transport rate (ETR); and (F) light mitochondrial non-photorespiratory respiration rate (R_{light}). Different letters indicate significant difference ($P \leq 0.05$) across all experimental conditions according to LSD test. $n=5$ in all cases.

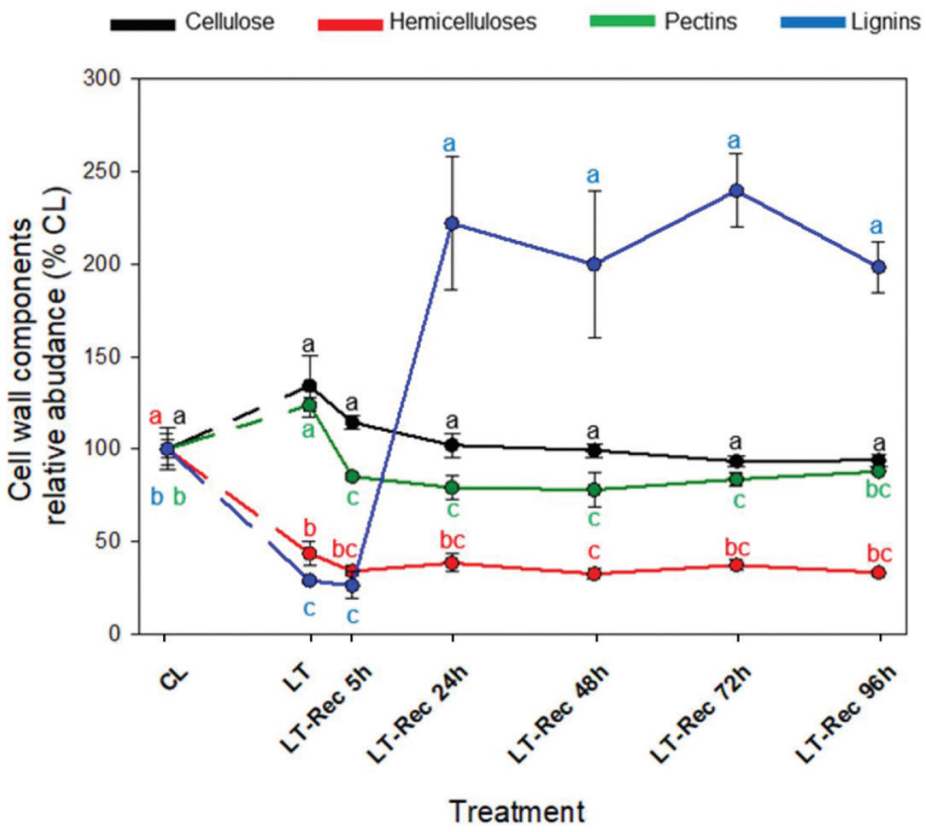

Fig. 6. Relative abundance of main cell wall components during LT and gradual LT-Rec application. Treatments' abbreviations correspond to CL: control; LT: long-term water deficit stress; LT-Rec 5 h, LT-Rec 24 h, LT-Rec 48 h, LT-Rec 72 h, and LT-Rec 96 h: long-term water deficit stress followed by 5, 24, 48, 72 and 96 h of recovery, respectively. Different letters indicate significant difference ($P \leq 0.05$) across all experimental conditions according to LSD test. n=5 (means ± SE).

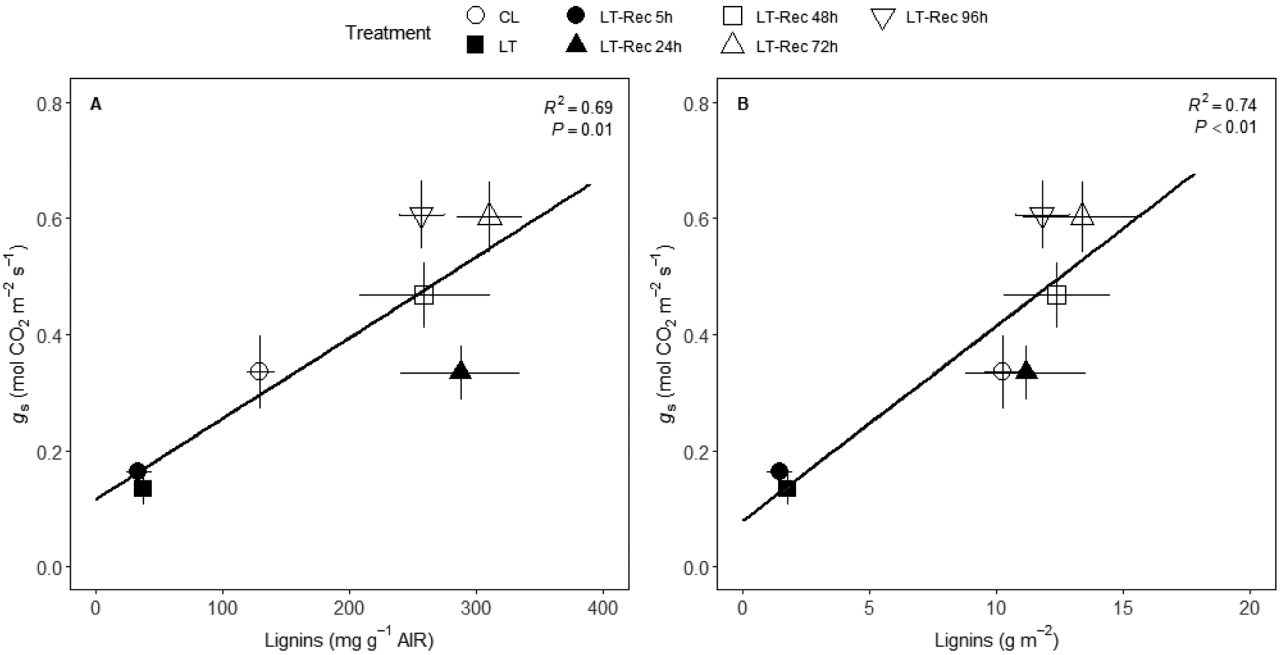

Fig. 7. Cell wall composition in relation to photosynthesis during long-term water deficit stress and gradual long-term water deficit stress followed by recovery. Relationship between stomatal conductance to gas diffusion (g_s) and lignins content expressed on an AIR basis (A) and on an area basis (B). n=5 (means ± SE).

absolute concentration which is expected to affect porosity (Flexas *et al.*, 2021). Instead, if the role of cell wall composition is related to affect the length of the CO_2 pathway, to express cell wall components on an area basis might be more relevant to link them with area-based traits such as photosynthesis and g_m. Whatever the case, different results were obtained in this study by expressing cell wall compounds on an area or on an AIR basis. Consequently, we will discuss our results from these two perspectives.

Cell wall composition of mature leaves expressed on an AIR basis is dynamically modified by different water availability conditions

By the application of gradual ST and LT-Rec treatments, we could examine in detail how changes in cell wall composition occurred, noting their high dynamics in mature leaves (Figs 2 and Figs 6). Gradual ST application resulted in enhanced relative content of pectins, reaching the highest value under ST-40% FC (Fig. 2). The fact that water deficit stress increases the amount of pectins has been widely described (Sweet *et al.*, 1990; Vicré *et al.*, 1999; 2004; Leucci *et al.*, 2008; Moore *et al.*, 2008; Clemente-Moreno *et al.*, 2019; Nadal *et al.*, 2020; Roig-Oliver *et al.*, 2020a, b, c) and this could reflect the importance of pectins in maintaining the degree of cell wall hydration during water deprivation, which may also imply alterations in wall flexibility and extensibility (Leucci *et al.*, 2008; Moore *et al.*, 2008; Tenhaken, 2015). This role for pectins has been proposed even in resurrection plants, which are able to withstand extreme dehydration due to modifications in physicochemical properties of pectins, as well as in their interactions with other cell wall components (Vicré *et al.*, 1999; 2004; Moore *et al.*, 2008). Similar to ST application and to those results that we previously reported (Roig-Oliver *et al.*, 2020a), higher pectins content was also detected under LT compared with CL, decreasing significantly after only 5 h upon recovery (Fig. 6). These results are of high relevance since most studies exploring the dynamics of cell wall modifications due to abiotic stresses focused on genetic and/or proteomic responses instead of compositional analyses, and did not address potential changes in time scales as short as those evaluated here (Tenhaken, 2015). Interestingly, lignins components which are mainly found in secondary cell walls – also displayed important variations in their relative abundance (Figs 2 and Figs 6), which could be potentially associated with alterations in cell wall strength, flexibility, and extensibility (Wallace and Fry, 1994; Terrett and Dupree, 2019). Vincent *et al.* (2005) and Terzi *et al.* (2013) reported that lignin content varied after days of water deficit stress application. However, as shown here, these modifications occurred more rapidly than expected and/or previously reported and were of especially large magnitude during gradual LT-Rec, particularly after 24 h of rewatering, suggesting high responsiveness of lignin biosynthesis to different water availability treatments.

The relationship between pectins and g_m during gradual short-term water deficit stress differs when expressed on an area or on an AIR basis

Some studies have recently demonstrated that changes in cell wall composition expressed on an AIR basis are related to photosynthesis, particularly via g_m, by testing mature leaves developed under well-watered conditions with subsequent acclimation to contrasting abiotic stresses (Clemente-Moreno *et al.*, 2019; Roig-Oliver *et al.*, 2020b, c). Although Roig-Oliver *et al.* (2020c) detected that changes in cellulose amounts were the main determinant of g_m responses in grapevines subjected to water deficit stress, growth chamber conditions, and Mediterranean summer for a month, species-specific adjustments emerged when comparing *G. biloba* and *H. annuus* submitted to water deprivation for 40 days (Roig-Oliver *et al.*, 2020b). However, here we found that modifications in pectins concentration negatively correlated with g_m modifications occurring during gradual ST (Fig. 3A), which agrees with the results reported by Clemente-Moreno *et al.* (2019) testing salt- and water-stressed tobacco for six days. Additionally, we observed for the first time that pectins are related to enhancement of the g_m/g_s ratio during gradual ST (Fig. 3B), providing some light on the mechanistic basis of the g_m/g_s ratio regulation, which remains largely unknown (Flexas *et al.*, 2013) . In fact, the g_m/g_s ratio positively correlates with WUE and could be crucial to simultaneously improve both photosynthesis and WUE in crops prone to be drought-affected, since g_m reflects the CO_2 diffusion and g_s accounts for both CO_2 and water diffusion towards inside the leaf and the atmosphere, respectively (Flexas *et al.*, 2013). Overall, we suggest that the application of ST treatments differing in their degree of water deprivation promoted accumulation of pectins, which could be accompanied by modifications in their physicochemical properties as well as in their interactions with other wall components, ultimately altering cell wall characteristics that affect CO_2 diffusion, such as porosity and thickness (Carpita *et al.*, 1979; Baron-Epel *et al.*, 1988; Franková and Fry, 2013; Lundgren and Fleming, 2020; Flexas *et al.*, 2021). However, as shown in Figs 3A, B, all the studies mentioned above showed relationships between g_m and cell wall composition expressing the amounts of a specific cell wall compound on an AIR basis. Nonetheless, contrasting conclusions could be reached when expressed on an area basis, since in this case no connection between pectins and g_m or the g_m/g_s ratio was observed (Figs 3C, D, respectively). The fact that these correlations emerge when expressed on an AIR basis but not when expressed on an area basis, may suggest that their role in determining g_m is mostly related to cell wall porosity than to total wall diffusion path length. However, this remains speculative until more direct approaches become available to test the specific role of each cell wall component affecting CO_2 diffusion.

The effect of lignins on g_s during gradual recovery preceded by a long-term water deficit stress when expressed either on an area or on an AIR basis

To the best of our knowledge, only the study by Roig-Oliver *et al.* (2020a) has previously examined the effect of LT and LT-Rec on cell wall composition and g_m by testing mature leaves developed under water shortage conditions. However, since in that study the number of different treatments was small, correlations among parameters were tested by pooling ST and LT data together. Nonetheless, the more in-depth study presented here suggests that LT plants may behave differently than ST ones. Surprisingly, the detailed LT-Rec monitoring that we performed showed that larger g_s achieved upon recovery was associated with enhancement in lignins amounts expressed on an AIR basis (Fig. 7A), and the strength of that correlation increased when lignins content was expressed on an area basis (Fig. 7B). Whilst Kuusk *et al.* (2018) reported that lignins did not directly affect photosynthesis, Roig-Oliver *et al.* (2020a) found that, when expressed on an AIR basis, they were almost significantly correlated with g_m combining data for sunflowers subjected to short- and long-term water deficit stresses followed by recoveries. Additionally, Coleman *et al.* (2008) observed that severe reductions of cell wall lignification in transgenic poplar trees were accompanied by a significant g_s decline, leading to the suggestion that changes in the cell wall composition of guard cells as well as in the functioning of specific wall enzymes could potentially affect stomatal movements (Gago *et al.*, 2016), even under water deficit stress (Choi *et al.*, 2011). Although more detailed studies are necessary to elucidate how specific changes in cell wall composition of guard cells could promote g_s adjustments, our results may indicate that even modifications in the overall leaf cell wall composition could have the potential to influence g_s since this relationship is detected either when expressing lignins on an area or on an AIR basis.

This study shows photosynthetic responses and a highly dynamic turnover of the main constituents of cell walls in mature *H. annuus* leaves subjected to different levels of water availability. Although further studies are necessary to re-evaluate and ameliorate the accuracy of the standard colorimetric procedures to quantify cell wall compounds, we show that changes in cell wall composition are distinctly related to photosynthesis across treatments. During gradual ST, whilst enhanced pectins content expressed on an AIR basis correlated with down-regulated g_m, this relationship was non-significant when expressing pectins on an area basis. In contrast, LT leaves did not show impaired g_m, and the detailed monitoring of LT-Rec reflected that photosynthesis was gradually increased from LT because of g_s and ETR enhancements. These photosynthetic changes occurring upon recovery were accompanied by fast modifications in the main composition of cell walls, with pectins and lignins being the fastest and most widely changing compounds, respectively. In particular, after only 5 h of rewatering, pectins were present at even lower concentrations than control, while lignins drastically increased (>200%) after 24 h, being associated with g_s increments, even when expressed on an area or on an AIR basis. Consequently, given that the observed responses for most of the traits differed between gradual ST as well as during LT and LT-Rec, further studies are required to test other species subjected to more conditions by using re-evaluated protocols to analyse cell wall composition accurately. This would elucidate the relevance of modifications in cell wall composition distinctly affecting photosynthesis.

Supplementary data

The following supplementary data are available at *JXB* online.

Fig. S1. Photosynthetic characterization of *H. annuus* plants gradually acclimated to different conditions.

Table S1. Leaf cell wall composition of *H. annuus* plants acclimated to different conditions.

Table S2. Leaf water status of *H. annuus* plants gradually acclimated to different conditions.

Table S3. Leaf cell wall composition of *H. annuus* plants gradually acclimated to different conditions.

Table S4. Pearson correlation matrix of photosynthetic, leaf water status, and cell wall parameters measured in *H. annuus* plants across ST experimental conditions.

Table S5. Pearson correlation matrix of photosynthetic, leaf water status, and cell wall parameters measured in *H. annuus* plants across LT and LT-Rec experimental conditions.

Acknowledgements

We thank Dr Mateu Fullana-Pericàs for his help with maintenance of plants and Dr Cyril Douthe for technical support during gas exchange measurements.

Author contributions

MR-O, JB, and JF designed the study; MR-O, PB, and DN conducted the experiments; MR-O and JF performed the data analysis, and MR-O wrote the first version of the manuscript with contributions of all co-authors.

Conflict of interest

The authors declare no conflicts of interest.

Funding

This work was supported by the project PGC2018-093824-B-C41 from Ministerio de Economía y Competitividad (MINECO, Spain) and the ERDF (FEDER). MR-O was supported by a predoctoral fellowship FPU16/01544 from MINECO.

Data availability

The data supporting the findings of this study are available from the corresponding author upon request.

References

Anderson CT, Kieber JJ. 2020. Dynamic construction, perception, and remodeling of plant cell walls. Annual Review of Plant Biology **71**, 39–69.

Baron-Epel O, Gharyal PK, Schindler M. 1988. Pectins as mediators of wall porosity in soybean cells. Planta **175**, 389–395.

Baskin TI. 2005. Anisotropic expansion of the plant cell wall. Annual Review of Cell and Developmental Biology **21**, 203–222.

Blumenkrantz N, Asboe-Hansen G. 1973. New method for quantitative determination of uronic acids. Analytical Biochemistry **54**, 484–489.

Caffall KH, Mohnen D. 2009. The structure, function, and biosynthesis of plant cell wall pectic polysaccharides. Carbohydrate Research **344**, 1879–1900.

Carpita NC, Gibeaut DM. 1993. Structural models of primary cell walls in flowering plants: consistency of molecular structure with the physical properties of the walls during growth. The Plant Journal **3**, 1–30.

Carpita NC, Sabularse D, Montezinos D, Delmer DP. 1979. Determination of the pore size of cell walls of living plant cells. Science **205**, 1144–1147.

Carriquí M, Nadal M, Clemente-Moreno MJ, Gago J, Miedes E, Flexas J. 2020. Cell wall composition strongly influences mesophyll conductance in gymnosperms. The Plant Journal **103**, 1372–1385.

Chaves MM, Flexas J, Pinheiro C. 2009. Photosynthesis under drought and salt stress: regulation mechanisms from whole plant to cell. Annals of Botany **103**, 551–560.

Chaves MM, Pereira JS, Maroco J, Rodrigues ML, Ricardo CP, Osório ML, Carvalho I, Faria T, Pinheiro C. 2002. How plants cope with water stress in the field. Photosynthesis and growth. Annals of Botany **89**, 907–916.

Choi JY, Seo YS, Kim SJ, Kim WT, Shin JS. 2011. Constitutive expression of CaXTH3, a hot pepper xyloglucan endotransglucosylase/hydrolase, enhanced tolerance to salt and drought stresses without phenotypic defects in tomato plants (*Solanum lycopersicum* cv. Dotaerang). Plant Cell Reports **30**, 867–877.

Clemente-Moreno MJ, Gago J, Díaz-Vivancos P, Bernal A, Miedes E, Bresta P, Liakopoulos G, Fernie AR, Hernández JA, Flexas J. 2019. The apoplastic antioxidant system and altered cell wall dynamics influence mesophyll conductance and the rate of photosynthesis. The Plant Journal **99**, 1031–1046.

Coleman HD, Samuels AL, Guy RD, Mansfield SD. 2008. Perturbed lignification impacts tree growth in hybrid poplar–a function of sink strength, vascular integrity, and photosynthetic assimilation. Plant Physiology **148**, 1229–1237.

Cosgrove DJ. 2005. Growth of the plant cell wall. Nature Reviews. Molecular Cell Biology **6**, 850–861.

Cosgrove DJ. 2018. Diffuse growth of plant cell walls. Plant Physiology **176**, 16–27.

De Lorenzo G, Ferrari S, Giovannoni M, Mattei B, Cervone F. 2019. Cell wall traits that influence plant development, immunity, and bioconversion. The Plant Journal **97**, 134–147.

Dubois M, Gilles KA, Hamilton JK, Rebers PA, Smith F. 1956. Colorimetric method for determination of sugars and related substances. Analytical Chemistry **28**, 350–356.

Fagerstedt KV, Saranpää P, Tapanila T, Immanen J, Serra JA, Nieminen K. 2015. Determining the composition of lignins in different tissues of silver birch. Plants **4**, 183–195.

Flexas J, Bota J, Loreto F, Cornic G, Sharkey TD. 2004. Diffusive and metabolic limitations to photosynthesis under drought and salinity in C_3 plants. Plant Biology **6**, 269–279.

Flexas J, Clemente-Moreno MJ, Bota J, *et al.* 2021. Cell wall thickness and composition are involved in photosynthetic limitation. Journal of Experimental Botany **72**, 3971–3986.

Flexas J, Niinemets U, Gallé A, *et al.* 2013. Diffusional conductances to CO_2 as a target for increasing photosynthesis and photosynthetic water-use efficiency. Photosynthesis Research **117**, 45–59.

Franková L, Fry SC. 2013. Biochemistry and physiological roles of enzymes that 'cut and paste' plant cell-wall polysaccharides. Journal of Experimental Botany **64**, 3519–3550.

Gago J, Daloso Dde M, Figueroa CM, Flexas J, Fernie AR, Nikoloski Z. 2016. Relationships of leaf net photosynthesis, stomatal conductance, and mesophyll conductance to primary metabolism: a multispecies meta-analysis approach. Plant Physiology **171**, 265–279.

Harley PC, Loreto F, Di Marco G, Sharkey TD. 1992. Theoretical considerations when estimating the mesophyll conductance to $CO_{(2)}$ flux by analysis of the response of photosynthesis to $CO_{(2)}$. Plant Physiology **98**, 1429–1436.

Houston K, Tucker MR, Chowdhury J, Shirley N, Little A. 2016. The plant cell wall: a complex and dynamic structure as revealed by the responses of genes under stress conditions. Frontiers in Plant Science **7**, 984.

Ibarz A, PagPa A, Tribaldo F, Pagba J. 2005. Improvement in the measurement of spectrophotometric data in the *m*-hydroxydiphenyl pectin determination methods. Food Control **17**, 890–893.

Iiyama K, Lam T, Stone BA. 1994. Covalent cross-links in the cell wall. Plant Physiology **104**, 315–320.

Kanevski I, Maliga P, Rhoades DF, Gutteridge S. 1999. Plastome engineering of ribulose-1,5-bisphosphate carboxylase/oxygenase in tobacco to form a sunflower large subunit and tobacco small subunit hybrid. Plant Physiology **119**, 133–142.

Keegstra K. 2010. Plant cell walls. Plant physiology **154**, 483–486.

Kent SS, Andre M, Cournac L, Farineau J. 1992. An integrated model for the determination of the Rubisco specificity factor, respiration in the light and other photosynthetic parameters of C_3 plants in situ. Plant Physiology and Biochemistry **30**, 625– 637.

Kuusk V, Niinemets Ü, Valladares F. 2018. A major trade-off between structural and photosynthetic investments operative across plant and needle ages in three Mediterranean pines. Tree Physiology **38**, 543–557.

Lampugnani ER, Khan GA, Somssich M, Persson S. 2018. Building a plant cell wall at a glance. Journal of Cell Science **131**: jcs207373.

Leucci MR, Lenucci MS, Piro G, Dalessandro G. 2008. Water stress and cell wall polysaccharides in the apical root zone of wheat cultivars varying in drought tolerance. Journal of Plant Physiology **165**, 1168–1180.

Lundgren MR, Fleming AJ. 2020. Cellular perspectives for improving mesophyll conductance. The Plant Journal **101**, 845–857.

Masuko T, Minami A, Iwasaki N, Majima T, Nishimura S, Lee YC. 2005. Carbohydrate analysis by a phenol-sulfuric acid method in microplate format. Analytical Biochemistry **339**, 69–72.

Moore JP, Farrant JM, Driouich A. 2008. A role for pectin-associated arabinans in maintaining the flexibility of the plant cell wall during water deficit stress. Plant Signaling & Behavior **3**, 102–104.

Moreira-Vilar FC, Siqueira-Soares Rde C, Finger-Teixeira A, de Oliveira DM, Ferro AP, da Rocha GJ, Ferrarese Mde L, dos Santos WD, Ferrarese-Filho O. 2014. The acetyl bromide method is faster, simpler and presents best recovery of lignin in different herbaceous tissues than Klason and thioglycolic acid methods. PloS One **9**, e110000.

Nadal M, Roig-Oliver M, Bota J, Flexas J. 2020. Leaf age-dependent elastic adjustment and photosynthetic performance under drought stress in *Arbutus unedo* seedlings. Flora **271**, 151662.

Niinemets Ü, Cescatti A, Rodeghiero M, Tosens T. 2005. Leaf internal diffusion conductance limits photosynthesis more strongly in older leaves of Mediterranean evergreen broadleaved species. Plant, Cell & Environment **28**, 1552–1566.

Novaković L, Guo T, Bacic A, Sampathkumar A, Johnson K. 2018. Hitting the wall – Sensing and signaling pathways involved in plant cell wall remodeling in response to abiotic stress. Plants **7**, 89.

Ochoa-Villarreal M, Aispuro-Hernández E, Vargas-Arispuro I, Martínez-Téllez MA. 2012. Plant cell wall polymers: function, structure and biological activity of their derivatives. In: De Souza Gomes A, ed. Polymerization. Rikeja, Croatia. InTechOpen. doi: 10.5772/2750.

Panković D, Sakač Z, Kevrešan S, Plesničar M. 1999. Acclimation to long-term water deficit in the leaves of two sunflower hybrids: photosynthesis,

electron transport and carbon metabolism. Journal of Experimental Botany **50**, 127–138.

Parry MAJ, Keys AJ, Gutteridge S. 1989. Variation in the specificity factor of C-3 higher plant Rubisco determined by the total consumption of ribulose-P-2. Journal of Experimental Botany **40**, 317–320.

Rancour DM, Marita JM, Hatfield RD. 2012. Cell wall composition throughout development for the model grass *Brachypodium distachyon*. Frontiers in Plant Science **3**, 266.

Roig-Oliver M, Bresta P, Nadal M, Liakopoulos G, Nikolopoulos D, Karabourniotis G, Bota J, Flexas J. 2020a. Cell wall composition and thickness affect mesophyll conductance to CO_2 diffusion in *Helianthus annuus* under water deprivation. Journal of Experimental Botany **71**, 7198–7209.

Roig-Oliver M, Nadal M, Bota J, Flexas J. 2020b. *Ginkgo Biloba* and *Helianthus annuus* show different strategies to adjust photosynthesis, leaf water relations, and cell wall composition under water deficit stress. Photosynthetica **58**, 1098–1106.

Roig-Oliver M, Nadal M, Clemente-Moreno MJ, Bota J, Flexas J. 2020c. Cell wall components regulate photosynthesis and leaf water relations of *Vitis vinifera* cv. Grenache acclimated to contrasting environmental conditions. Journal of Plant Physiology **244**, 153084.

Rui Y, Dinneny JR. 2019. A wall with integrity: surveillance and maintenance of the plant cell wall under stress. New Phytologist **225**, 1428–1439.

Sahaf M, Sharon E. 2016. The rheology of a growing leaf: stress-induced changes in the mechanical properties of leaves. Journal of Experimental Botany **67**, 5509–5515.

Sharwood RE, von Caemmerer S, Maliga P, Whitney SM. 2008. The catalytic properties of hybrid Rubisco comprising tobacco small and sunflower large subunits mirror the kinetically equivalent source Rubiscos and can support tobacco growth. Plant Physiology **146**, 83–96.

Sweet WJ, Morrison JC, Labavitch J, Matthews MA. 1990. Altered synthesis and composition of cell wall of grape (*Vitis vinifera* L.) leaves during expansion and growth-inhibiting water deficits. Plant and Cell Physiology **31**, 407–414.

Tenhaken R. 2015. Cell wall remodeling under abiotic stress. Frontiers in Plant Science **5**, 771.

Terrett OM, Dupree P. 2019. Covalent interactions between lignin and hemicelluloses in plant secondary cell walls. Current Opinion in Biotechnology **56**, 97–104.

Terzi R, Guler NS, Caliş̧kan N, Kadioğlu A. 2013. Lignification response for rolled leaves of *Ctenanthe setosa* under long-term drought stress. Turkish Journal of Biology **37**, 614–619.

Tucker MR, Lou H, Aubert MK, Wilkinson LG, Little A, Houston K, Pinto SC, Shirley NJ. 2018. Exploring the role of cell wall-related genes and polysaccharides during plant development. Plants **7**, 42.

Uddin MN, Hanstein S, Faust F, Eitenmüller PT, Pitann B, Schubert S. 2014. Diferulic acids in the cell wall may contribute to the suppression of shoot growth in the first phase of salt stress in maize. Phytochemistry **102**, 126–136.

Valentini R, Epron D, Angelis PD, Matteucci G, Dreyer E. 1995. In situ estimation of net CO_2 assimilation, photosynthetic electron flow and photorespiration of Turkey oak (*Q. cerris* L.) leaves: diurnal cycles under different water supply. Plant, Cell & Environment **18**, 631–64.

Vicré M, Lerouxel O, Farrant J, Lerouge P, Driouich A. 2004. Composition and desiccation-induced alterations of the cell wall in the resurrection plant *Craterostigma wilmsii*. Physiologia Plantarum **120**, 229–239.

Vicré M, Sherwin HW, Driouich A, Jaffer MA, Farrant JM. 1999. Cell wall characteristics and structure of hydrated and dry leaves of the resurrection plant *Craterostigma wilsmii*, a microscopical study. Journal of Plant Physiology **155**, 719–726.

Vincent D, Lapierre C, Pollet B, Cornic G, Negroni L, Zivy M. 2005. Water deficits affect caffeate O-methyltransferase, lignification, and related enzymes in maize leaves. A proteomic investigation. Plant Physiology **137**, 949–960.

Wallace G, Fry SC. 1994. Phenolic components of the plant cell wall. International Review of Cytology **151**, 229–267.

Weraduwage SM, Campos ML, Yoshida Y, *et al.* 2018. Molecular mechanisms affecting cell wall properties and leaf architecture. In: AdamsIII W, Terashima I, eds. The leaf: a platform for performing photosynthesis. Advances in Photosynthesis and Respiration (Including Bioenergy and Related Processes), vol 44. Springer International Publishing, Cham, Switzerland.